http://dx.doi.org/10.5516/NET.09.2014.718

EFFECTS OF MECHANICAL PROPERTY VARIABILITY IN LEAD RUBBER BEARINGS ON THE RESPONSE OF SEISMIC ISOLATION SYSTEM FOR DIFFERENT GROUND MOTIONS

YOUNG-SUN CHOUN*, JUNHEE PARK, and IN-KIL CHOI
Korea Atomic Energy Research Institute
989-111 Daedeok-daero, Yuseong-gu, Daejeon 305-353, Republic of Korea
*Corresponding author. E-mail : sunchun@kaeri.re.kr

Received September 29, 2014

The effects of variability of the mechanical properties of lead rubber bearings on the response of a seismic isolation system are investigated. Material variability in manufacturing, aging, and operation temperature is assumed, and two variation models of an isolation system are considered. To evaluate the effect of ground motion characteristics on the response, 27 earthquake record sets with different peak A/V ratios were selected, and three components of ground motions were used for a seismic response analysis. The response in an isolation system and a superstructure increases significantly for ground motions with low A/V ratios. The variation in the mechanical properties of isolators results in a significant influence on the shear strains of the isolators and the acceleration response of the superstructure. The variation provisions in the ASCE-4 are reasonable, but more strict variation limits should be given to isolation systems subjected to ground motions having low A/V ratios. For application of seismic isolation systems to safety-related nuclear structures, the variation in the material and mechanical properties of the isolation system should be properly controlled during the manufacturing and aging processes. In addition, special consideration should be given to minimize the accidental torsion caused by the dissimilarity in the stiffness variations of the isolators.

KEYWORDS : Seismic Isolation, Stiffness Variability, Peak A/V Ratio, Lead Rubber Bearing, Mechanical Property, Eccentricity

1. INTRODUCTION

The basic concept of seismic base isolation is to introduce a flexible layer between the base floor of a superstructure and the foundation system to reduce damage to the superstructure during earthquake ground motions. The flexible layer in the horizontal plane is capable of permitting a large lateral displacement, and thus decoupling the superstructure from the horizontal components of ground motions. Since the behavior of an isolation system and a superstructure greatly depends on the mechanical properties of the isolation devices, a deep understanding of the characteristics of isolation devices is essential for designing seismic isolation systems.

An isolation rubber bearing consists of alternating rubber layers bonded between thin steel plates to provide lateral flexibility. The internal steel plates reduce the lateral bulging of the bearing, and provide a much higher vertical stiffness than the horizontal stiffness. The natural rubber bearings show a linear behavior in shear up to shear strains above 100%, and have damping in the range of 2-3% of critical [1]. Lead-rubber bearings (LRBs) have one or more lead plugs that are inserted into holes in a low-damping natural rubber bearing to increase the damping capacity. Under lateral deformation, the lead plug deforms in almost pure shear, yields at low levels of stress and at normal temperatures, and produces hysteretic behavior that is stable over many cycles. The lead plug recrystallizes under normal temperatures, and thus repeated yielding does not cause fatigue failure. LRBs generally exhibit a characteristic strength that ensures rigidity under service loads [2]. Because the steel plates in a laminated rubber bearing force the lead plug to deform in shear, the behavior of LRB may be represented through a bilinear model, which can be characterized with three parameters: the initial stiffness, post-yield stiffness, and characteristic strength.

The mechanical properties of isolation rubber bearings, i.e., stiffness and characteristic strength, are influenced by aging, environmental effects, temperature, and other effects. Since the rubber bearings have an inherent variability in their mechanical properties owing to the variability in rubber materials and manufacturing processes, the stiffness and damping values of the bearings used for construction must be different from those values used for the design. In practice, the mass distribution of superstructures at the floor level, and the stiffness distribution of base-isolated systems, can be irregular. For this reason, the actual eccentricity between the mass center of a superstructure and the stiffness center of an isolation system can be different from the eccentricity used for the analysis and design. Therefore, most of the real base-isolated buildings are asymmetrical. Accidental eccentricity, due to discrepancies between the distributions of mass and stiffness in the design and true distributions at the time of an earthquake, can create torsional coupling during the ground excitations [3].

The variability in the stiffness and damping of the isolation system generates uncertainty in the lateral and torsional vibration periods, and creates additional lateral-torsional coupling [3]. Llera and Inaudi [3] investigated the increase in building response due to stiffness uncertainty in base-isolated systems. It was found that the increase in response resulting from stiffness uncertainty is very sensitive to the frequency ratio between the nominal values of the uncoupled torsional and lateral frequencies of the system, and the number of isolators. The increase in isolator displacements at the building edge reaches a peak at the frequency ratio of 1.2 and rarely exceeds 10%. The value decreases for buildings with a larger number of isolators. Jangid and Kelly [4] studied the effects of torsional coupling on the seismic response of a base-isolated building. It was shown that torsional coupling can influence the response of the isolated structure, but if the layout of the isolation bearings is such that the torsional frequency is larger than the lateral frequency, the effect is reduced. They recommended that the torsional frequency be 1.2-times greater than the lateral frequency of the isolated system. Nagarajaiah, et al. [5] studied torsion in base-isolated structures with inelastic elastomeric isolation systems due to bidirectional lateral ground motion. Their conclusions are as follows: (a) the main source of torsional motions in elastomeric isolated structures is the isolation system eccentricity, (b) increasing isolation eccentricity leads to increased torque amplification, (c) an accidental isolation eccentricity of 5% may result in significant torque amplification, and (d) increasing the isolation eccentricity with decreasing ratios of torsional-to-lateral frequencies for the superstructure and base generally leads to increased corner-displacement magnifications. Tena-Colunga and Zambrana-Rojas [6] concluded that the main source of torsional motions in elastomeric isolated structures seems to be the isolation system eccentricity, particularly when the eccentricity is large (greater than 10%). However, this observation needs to be confirmed through more detailed studies. Matsagar and Jangid [7] evaluated the effects of torsional coupling, due to the isolator parameters, on the seismic response of base-isolated buildings. They concluded that the eccentricities arising from the dissimilar isolator properties in the base-isolated building have a major influence on the displacement response, and in presence of such isolation eccentricities, the eccentricity of a superstructure is not important.

The response of structural systems with a low natural frequency, such as seismically isolated structures, is very sensitive to the frequency content of the input ground motions. To investigate the effect of the frequency content of input ground motions on the seismic response, the peak ground acceleration to velocity (A/V) ratio has been utilized [8-10]. The ground motions exhibiting a large amplitude and very high frequency content generally result in high A/V ratios, while the ground motions containing intense and long duration acceleration pulses will generally lead to low A/V ratios.

This paper investigates the effect of variability in the mechanical properties of LRBs on the seismic response of base isolation systems subjected to input ground motions with different peak A/V ratios. Variability in manufacturing, aging, and temperature was examined, and a seismic response analysis for a base isolated nuclear island was conducted for earthquake ground motions having different peak A/V ratios. An ideal model, where variation in the material properties of individual isolators is identical, and an eccentric model, where eccentricity in one direction is created owing to different variations in the material properties of the isolators, are used to consider the dissimilarity of variations in individual isolators.

2. VARIABILITY IN MECHANICAL PROPERTIES OF RUBBER BEARINGS

2.1 Variability in Manufacturing Process

The variability in the mechanical properties of isolation rubber bearings may be generated by the variation of rubber materials and the manufacturing tolerances in the manufacture process. The variability of the rubber materials is relatively higher than other structural materials because rubber is a viscoelastic material that has various responses due to a change in ingredients.

In manufacturing a rubber material, the raw material has to be admixed with a vulcanizing agent (i.e., sulfur), and other particular ingredients to make a more suitable material [11]. The ingredients include accelerators, activators, antioxidants, fillers and reinforcing agents, processing oils, retardants, softeners, and coloring additives. Their percentages used in a rubber compound are closely related to the properties of the rubber material to be achieved. Variations in the material properties of rubber can result

from variations in mixing and curing.

The manufacturing process is generally different for small- and large-size rubber bearings. Small-size bearings can be made using injection molding. Heated mixed rubber is injected from the perimeter into the mold and kept under pressure during the curing process [12]. Bearings made using this process can have inferior bond strength between the rubber layers and steel shim plates because the rubber moves from the exterior toward the interior during the injection process and can partially remove the adhesive. However, the advancement in techniques used in manufacturing has resulted in improvements in rubber compounds and their bonding to steel shims [11]. Large-size bearings are made in several steps: sheeting of rubber, cutting of rubber and steel plates, surface treatment of steel plates, coating adhesives, assembly of steel plates and rubber sheets, curing under pressure and heat, and inserting the lead plug.

Variations in the mechanical properties of the bearings, which depend on the experience of the manufacturer and the size of the bearing, may be generated from variations in the manufacturing process. Tolerances in manufacturing rubber bearings are provided by manufacturers, but the manufacturing tolerances for buildings are specified in the ISO standard [13].

2.2 Variability Due to Aging and Environmental Effects

Aging and environmental effects are important parameters that affect the mechanical properties of rubber bearing systems. During the lifetime of isolation systems, the mechanical properties of rubber bearings will be constantly changed by the vulcanization and degradation of the rubber due to environmental and chemical factors such as the thermal oxidation, ultraviolet irradiation, and ozone [14]. The significance of each degradation factor varies with respect to the loading and environmental conditions. Usually, thermal oxidation is the most significant degradation factors during the lifetime of natural rubber. Thermal oxidation hardens the rubber and results in a significant drop in performance [15]. A combination of degradation factors causes greater or lesser effects than the sum of the individual effects because of a synergistic effect.

Aging effects have been investigated for rubber bearings installed in bridges, buildings, and nuclear power plants [16-20]. The aging effects on the laminated rubber bearings of Pelham Bridge in England, which was constructed in 1957 and has been used for about 40 years, were investigated [16]. The major changes in the physical properties of the rubber material were limited to a depth of about 50 mm from the surface, and the horizontal stiffness increased by about 10% compared with the design value.

The aging effects on twenty two-year old natural rubber bearings, which were used in a seismically isolated three-story dormitory building, were evaluated [17]. The horizontal stiffness for shear strains of 10% and 50%, and 10% and 100%, decreased over both 10 and 22 years, respectively, whereas the values for shear strains of 10% and 200% increased about 7% in 10 years and 12% in 22 years. The vertical stiffness after 10 and 22 years of service increased about 16-19% and 13-15% compared to initial values, respectively. The aging of LRBs installed in a building for 15 years was investigated [18]. The compression stiffness increased approximately 15 to 23% and the shear stiffness increased up to about 9%; however, the yield force increased 0.7 to 3% in 15 years.

The aging of neoprene bearings used in the Cruas-Messye nuclear power plant was investigated. After 7 and 27 years, the shear modulus of the bearings was found to have increased by approximately 25% and 37% compared with the reference values at the manufacturing stage, respectively [19, 20]. Variations of damping with time were not clearly explained, but they were not significant.

It can be observed that the horizontal stiffness of rubber bearings increases about 10% after 15 to 40 years of service. AASHTO [21] suggested an aging factor of 1.1 for the post-yield stiffness in LRBs.

2.3 Variability Due to Temperature Effect

The mechanical properties of rubber bearings are influenced by ambient temperatures and the duration of exposure to these temperatures. Low temperatures increase the stiffness and strength of rubber bearings. The effect of low temperature appears to be instantaneous thermal and crystallization stiffening. Crystallization stiffening causes material stiffening with time because of the reorientation of its molecular structure [22, 23]. The temperature-dependent mechanical properties for LRBs can be estimated by [24]

$$\text{Characteristic strength: } Q_{d,t} = 1.146e^{-0.00879t} \cdot Q_{d,15} \quad (1)$$

$$\text{Post-yield stiffness: } K_{d,t} = 1.041e^{-0.00271t} \cdot K_{d,15} \quad (2)$$

where t is the temperature in °C, and $Q_{d,15}$ and $K_{d,15}$ are the characteristic strength and post-yield stiffness at 15°C, respectively.

System property modification factors accounting for the effects of temperature on the properties of LRBs and high-damping rubber bearings are listed in Reference [23]. For safety-related nuclear structures, the mechanical properties of isolators shall not vary over the lifespan by more than ±20% from the values used for the analysis and design, with 95% probability, accounting for variations in material properties at the time of isolator construction, aging, operating temperature, and creep. In addition, the isolation system shall be maintained at a temperature between 4.4°C (40°F) and 26.7°C (80°F) [25].

3. RESPONSES OF SEISMIC ISOLATION BEARINGS WITH VARIABILITY: CASE STUDY

3.1 Structural Model

The structural model for a nuclear island that is supported by the base isolation system is depicted in Fig. 1. The superstructure was represented by a lumped-mass stick model, in which the mass of each floor includes the mass of the walls, slabs, columns, and heavy equipment. The nuclear island and the base mat were modeled by solid elements. The fundamental periods of the structural model in the orthogonal directions are $T_x = T_y = 2.48$s. The base isolation system consists of 454 LRBs. The LRBs were designed to have an outside diameter of 1,500 mm and a height of 300 mm, with 10 layers of 11 mm thick rubber and a lead core diameter of 250 mm. The effective horizontal stiffness of a bearing is 7.68 kN/mm and the vertical stiffness is 76.76 kN/mm, which is ten-times that of the horizontal stiffness. A standard design response spectrum defined in the Regulatory Guide 1.60 [26] was employed, and a peak ground acceleration (PGA) of 0.5g was used for the seismic design. The horizontal displacement limit at the base isolation level was assumed to be 150 mm.

To investigate the effect of the variability in the mechanical properties of the isolation bearings on the earthquake response, two variation models were adopted: (1) an ideal model (Fig. 1(b)), where variations in the mechanical properties of individual isolators are identical, and (2) an eccentric model (Fig. 1(c)), where eccentricity in one direction is created due to different variations in the mechanical properties of the isolators for two regions. In Fig. 1(c), the shaded region has increased properties, and the other region has decreased properties. The eccentricity in the base isolation system will occur due to a discrepancy in the center of the mass of the superstructure (CM_s), and the center of rigidity in the base isolation system (CR_i). The stiffness eccentricity of the isolation system creates a lateral-torsional coupling mode.

The nonlinear behavior of LRBs was modeled by a bilinear model based on three parameters K_1, K_2, and Q, as presented in Fig. 1(d). The parameter values used to define the bilinear model are 51.59 kN/mm for the initial stiffness (K_1), 5.16 kN/mm for the post-yield stiffness (K_2), and 380 kN for the characteristic strength (Q). The horizontal and vertical behaviors of the isolation bearing were modeled based on the bilinear model and linear model, respectively.

3.2 Input Ground Motions

To evaluate the response of seismically isolated structures for earthquake ground motions with different frequency contents, 27 earthquake record sets with different peak A/V ratios were selected [27]. The data-set was obtained from 12 different earthquake events with magnitudes ranging from 5.25 to 7.6. The following acceleration records were used: (1) 1933 Long Beach (M_w = 6.3), (2) 1934 Lower (M_w = 6.5), (3) 1935 Helena (M_w = 6), (4) 1940 Imperial Valley (M_w = 6.6), (5) 1952 Kern

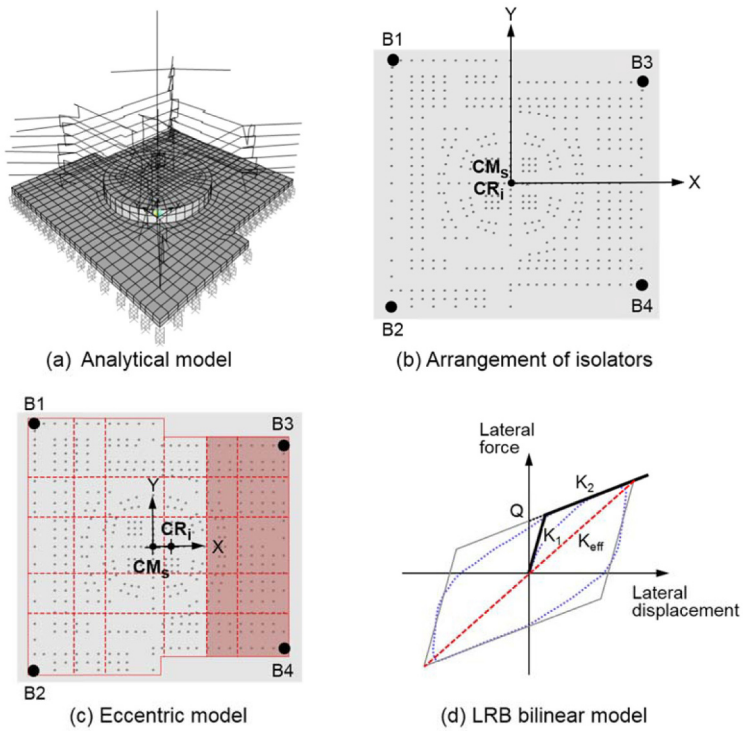

Fig. 1. Structural Models for Case Study

County (M_w = 7.6), (6) 1957 San Francisco (M_w = 5.25), (7) 1966 Parkfield (M_w = 5.6), (8) 1968 Borrego Mountain (M_w = 6.5), (9) 1970 Lytle Creek (M_w = 5.4), (10) 1971 San Fernando (M_w = 6.4), (11) 1975 Oroville (M_w = 5.7), and (12) 1985 Nahani (M_w = 7.5). The selected records have epicentral distances ranging from 4 to 131 km, PGAs ranging from 0.012 to 1.171g, and peak A/V ratios from 0.37 to 3.01 g/m/s. Table 1 shows the characteristics of the selected earthquake records with different peak A/V ratios: low A/V ratios (A/V < 0.8), intermediate A/V ratios (0.8 < A/V < 1.2), and high A/V ratios (A/V > 1.2). Two horizontal components (X and Y) and one vertical component of the ground motions were used for a seismic response analysis.

Normalized spectral accelerations for ground motions with different peak A/V ratios are plotted in Fig. 2. The ground motions containing low-frequency contents will generally lead to low A/V ratios, while the ground motions exhibiting large amplitude, very high frequency content in strong motions generally result in high A/V ratios. The normal ground motions, with significant energy content over a broad range of frequencies, will generally have intermediate A/V ratios, and their acceleration spectra are similar to the standard design response spectrum, as shown in the dotted line in Fig. 2. To prepare the ground motion input sets, the whole ensemble of 27 earthquake records in Table 1 was scaled to PGA = 0.5g.

Table 1a. Characteristics of Earthquake Ground Motions with Low A/V Ratios (A/V < 0.8)

No.	Earthquake Event	Station	X-component			Y-component			Soil Condition
			Max. Acc. (g)	Max. Vel. (m/s)	A/V (g/m/s)	Max. Acc. (g)	Max. Vel. (m/s)	A/V (g/m/s)	
1	Long Beach, CA	Subway Terminal, LA	0.098	0.237	0.41	0.064	0.173	0.37	Rock
2	San Fernando, CA	2500 Wilshire Blvd., LA	0.101	0.193	0.52	0.098	0.150	0.66	Stiff soil
3	San Fernando, CA	4680 Wilshire Blvd., LA	0.117	0.215	0.54	0.084	0.209	0.40	Stiff soil
4	San Fernando, CA	3470 Wilshire Blvd., LA	0.114	0.186	0.61	0.136	0.223	0.61	Stiff soil
5	San Fernando, CA	3550 Wilshire Blvd., LA	0.132	0.216	0.61	0.157	0.175	0.89	Stiff soil
6	San Fernando, CA	Hollywood Storage LA	0.106	0.170	0.62	0.151	0.194	0.78	Stiff soil
7	San Fernando, CA	445 Figueroa St., LA	0.119	0.173	0.69	0.150	0.173	0.87	Rock
8	San Fernando, CA	222 Figueroa St., LA	0.129	0.186	0.69	0.152	0.180	0.85	Stiff soil
9	Lower CA	El Centro	0.160	0.209	0.77	0.184	0.200	0.92	Stiff soil

Table 1b. Characteristics of Earthquake Ground Motions with Intermediate A/V Ratios (0.8 < A/V < 1.2)

No.	Earthquake Event	Station	X-component			Y-component			Soil Condition
			Max. Acc. (g)	Max. Vel. (m/s)	A/V (g/m/s)	Max. Acc. (g)	Max. Vel. (m/s)	A/V (g/m/s)	
1	San Fernando, CA	San Onofre SCE Power Plant	0.012	0.015	0.83	0.017	0.017	0.97	Stiff soil
2	San Fernando, CA	Griffith Park Observatory, LA	0.180	0.205	0.88	0.171	0.144	1.18	Rock
3	San Fernando, CA	3407 6th Street, LA	0.165	0.166	0.99	0.182	0.286	0.64	Stiff soil
4	San Fernando, CA	Hollywood Storage P.E., LA	0.211	0.211	1.00	0.187	0.279	0.67	Stiff soil
5	San Fernando, CA	3838 Lankershim Blvd., LA	0.151	0.149	1.01	0.167	0.120	1.39	Rock
6	Kern County, CA	Taft Lincoln School Tunnel	0.179	0.177	1.01	0.156	0.157	0.99	Rock
7	Imperial Valley	El Centro	0.348	0.334	1.04	0.214	0.369	0.58	Stiff soil
8	Borrego Mountain, CA	San Onofre SCE Power Plant	0.041	0.037	1.11	0.046	0.042	1.11	Stiff soil
9	San Fernando, CA	234 Figueroa Street LA	0.200	0.167	1.19	0.192	0.183	1.05	Stiff soil

Table 1c. Characteristics of Earthquake Ground Motions with High A/V Ratios (A/V > 1.2)

No.	Earthquake Event	Station	X-component			Y-component			Soil Condition
			Max. Acc. (g)	Max. Vel. (m/s)	A/V (g/m/s)	Max. Acc. (g)	Max. Vel. (m/s)	A/V (g/m/s)	
1	San Francisco, CA	State Bldg., S.F.	0.085	0.051	1.69	0.056	0.040	1.39	Stiff soil
2	San Fernando CA	Lake Hughes, Station 4	0.146	0.085	1.72	0.145	0.133	1.09	Rock
3	Parkfield, CA	Temblor No. 2	0.270	0.145	1.86	0.356	0.229	1.56	Rock
4	San Fernando, CA	Pacoima Dam	1.076	0.577	1.86	1.171	1.135	1.03	Rock
5	Oroville, CA	Seismograph Station	0.084	0.044	1.89	0.092	0.035	2.68	Rock
6	Helena, Montana	Carroll College	0.147	0.072	2.03	0.171	0.057	3.01	Rock
7	Lytle Creek	Wrightwood, CA	0.198	0.096	2.06	0.142	0.089	1.60	Rock
8	San Francisco, CA	Golden Gate Park	0.105	0.046	2.27	0.092	0.038	2.41	Rock
9	Nahani, Canada	Site 1, Iverson	1.101	0.462	2.38	0.978	0.457	2.14	Rock

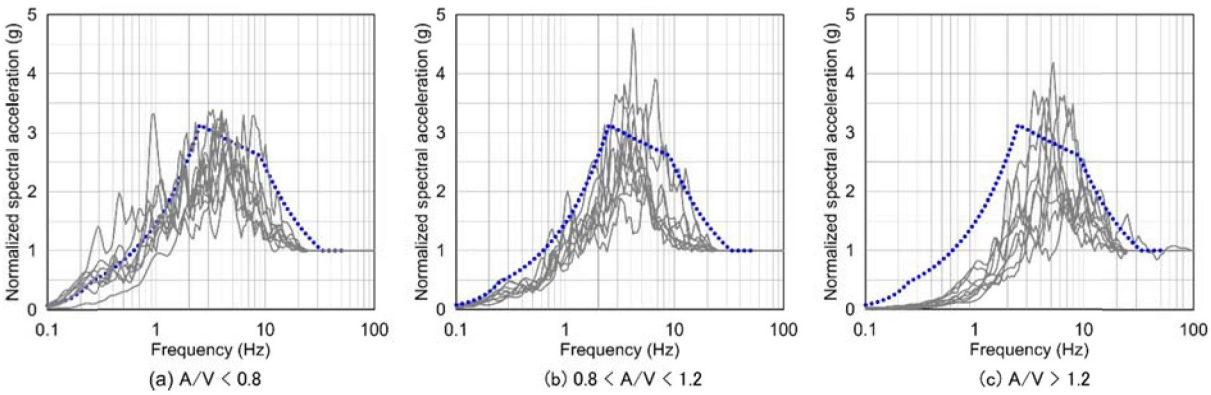

Fig. 2. Normalized Spectral Accelerations for Ground Motion Inputs (X- Component)

3.3 Mechanical Property Variability Considered

For seismically isolated, safety-related nuclear structures, ASCE-4 [25] requires a demonstration in which the mechanical properties of the isolators do not change by more than 20% over a 50- to 100-year period in the temperature range of 4.4°C (40°F) to 26.7°C (80°F). Over the lifespan of the nuclear structures, the greatest variability considered for isolator properties is restricted within ±20%, with 95% probability, accounting for all variations in material properties during manufacturing, construction, and long-term operation. Excluding variations in the operation temperatures, manufacturers have suggested that the variation limits in the manufacturing and aging of LRBs are ±10% and +10%, respectively [28]. This study assumed variations of ±10% for manufacturing and +10% for aging in the post-yield stiffness of the LRB bilinear model. For variations in the operation temperatures, the post-yield stiffness and characteristic strength were estimated using Eqs. (1) and (2) at 5°C and 25°C.

3.4 Seismic Responses of Isolators and Superstructures

As a result of the seismic response analysis for the ideal model shown in Fig. 1(b), the maximum displacements in the four corner isolators, B1, B2, B3, and B4, are summarized in Table 2. It can be seen that the maximum displacements for ground motions with high A/V ratios (A/V > 1.2) are all smaller than the design displacement of 15 cm, while those for ground motions with low and intermediate A/V ratios (A/V < 1.2) are larger than the design displacement. In particular, when a peak A/V ratio is lower than approximately 0.6 g/m/s, significant displacements are

Table 2. Maximum Displacements at the Top of Isolators in Ideal Model (cm)

EQ	A/V < 0.8		0.8 < A/V < 1.2		A/V > 1.2	
	Lateral Displ.	Vector Sum	Lateral Displ.	Vector Sum	Lateral Displ.	Vector Sum
1	57.97	60.03	10.45	10.60	3.50	4.03
2	32.58	34.01	10.85	11.43	5.62	6.18
3	27.27	32.16	11.41	13.01	3.21	3.51
4	20.95	25.03	17.24	17.24	0.86	1.02
5	17.07	19.60	2.91	3.14	3.46	4.52
6	25.36	25.46	12.58	15.23	9.93	10.16
7	18.16	18.28	15.70	16.60	2.43	2.51
8	7.72	7.94	13.08	14.44	3.59	4.96
9	8.73	8.81	12.33	12.47	2.90	3.15

Table 3. Maximum Displacements for Lower and Upper Bounds in Variation at the Top of Isolators (cm)

EQ	Lower Bound in Variation, -20%						Upper Bound in Variation, +20%					
	A/V < 0.8		0.8 < A/V < 1.2		A/V > 1.2		A/V < 0.8		0.8 < A/V < 1.2		A/V > 1.2	
	Lateral Displ.	Vector Sum	Lateral Displ.	Vector Sum	Lateral Displ.	Vector Sum	Lateral Displ.	Vector Sum	Lateral Displ.	Vector Sum	Lateral Displ.	Vector Sum
1	59.75	64.16	10.49	10.64	3.72	4.29	52.25	53.10	10.33	10.50	3.21	3.65
2	35.21	39.57	12.92	13.36	5.74	6.31	28.12	29.42	9.05	9.82	5.48	6.02
3	36.41	40.66	13.17	15.03	3.39	3.72	22.09	28.03	9.57	10.97	3.14	3.57
4	26.42	27.74	19.75	19.79	0.88	1.06	20.10	21.89	14.62	15.16	0.83	0.99
5	21.91	22.77	3.10	3.10	3.57	4.68	14.78	17.75	3.00	3.20	3.36	4.39
6	29.79	29.82	13.72	16.79	10.36	10.57	21.02	22.59	11.63	13.91	9.56	9.81
7	21.32	21.57	17.31	18.88	2.43	2.53	14.83	14.90	13.73	14.38	2.42	2.48
8	7.98	8.07	13.78	15.06	4.46	6.17	7.33	7.71	12.88	13.89	3.07	4.27
9	8.74	8.75	13.95	14.25	3.17	3.21	8.66	8.84	10.74	11.36	2.80	3.02

obtained because the ground motions are rich in low-frequency contents, as shown in Fig. 2(a). If the clearance distance of the moat walls is determined by a factor of 3 [29], the base-isolated structure can contact or impact moat walls for ground motions with low A/V ratios. For earthquake ground motion #1 (EQ #1) in low A/V ratios shown in Table 1a, whose peak A/V ratios are 0.41 g/m/s in the X-component and 0.37 g/m/s in the Y-component, the maximum lateral displacement obtained is approximately 58 cm, which is greater than the assumed moat wall gap of 45 cm.

Table 3 shows the maximum displacements in the four corner isolators for the lower and upper bounds in variation. According to the limit of variation in the mechanical properties of the isolators, given by ASCE-4 [25], stiffness variations of ±20% were applied. When all of the isolation bearings have a lower bound in stiffness variation, i.e., -20%, the maximum displacements (i.e., vector sum) of the isolators increase up to 26%, 17%, and 24% for A/V < 0.8, 0.8 < A/V < 1.2, and A/V > 1.2, respectively. The ratios of peak displacements to design displacement are plotted in Fig. 3. The ratios are smaller than 1.0 for A/V > 1.2, but they are amplified up to 4 for A/V < 0.8. In addition, the lower and upper bounds are almost the same for A/V > 1.2, but considerably different for A/V < 0.8. It can be seen that the displacement of the isolation system is significant for ground motions with low A/V ratios, and the effect of the stiffness variation of

the isolators on the displacement of the isolation system is highly sensitive to peak A/V ratios of the ground motions.

Fig. 4 shows the maximum shear strains in isolation bearings for their stiffness variations of ±20%. For A/V > 1.2, the maximum shear strains are smaller than 100%, while for A/V < 0.8, the maximum shear strains are obtained by more than 300%. In particular, the maximum shear strain for EQ #1 in low A/V reaches about 600%. In this huge shear strain, the rubber bearings must be destroyed, because the shear failure strain of typical rubber bearings is smaller than 500%. The stiffness variations of an isolation system can cause damage to the isolators during ground motions with low A/V ratios.

The stiffness variation of an isolation system also influences the response of the superstructure. Figs. 5 and 6 show the peak acceleration and relative displacement at the top of the superstructure, respectively. The response of superstructure increases significantly for ground motions with low A/V ratios. For EQ #1 in low A/V, the peak acceleration at the top of the superstructure is amplified as 0.41g. The peak accelerations and relative displacements for A/V < 0.8 are increased by more than twice the response for A/V > 0.8. It was revealed that the response of the isolation system is increased by the lower limit in variations, while the response of the superstructure is increased by the upper limit in variations. The upper limit in the stiffness variation of the isolators can diminish the decoupling performance of the isolation system.

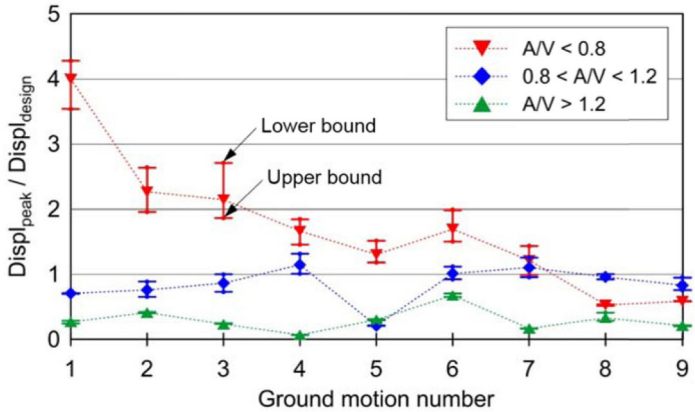

Fig. 3. Displacement Ratios for Lower and Upper Bounds in Variation of Isolators

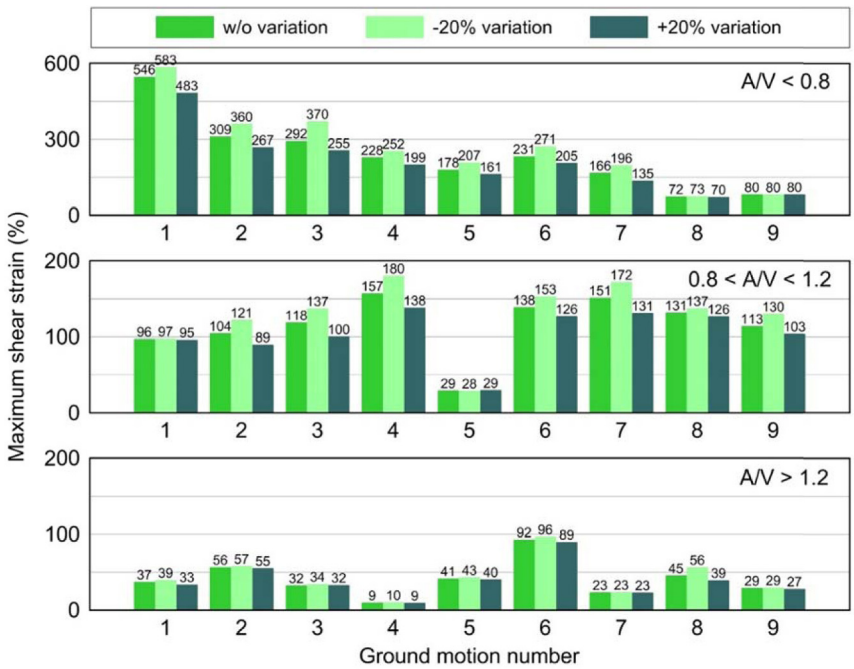

Fig. 4. Maximum Shear Strains of Isolators for Stiffness Variations

Fig. 7 shows the acceleration time-history at the top of the superstructure, and the displacement time-history at the top of isolator for EQ #1 in low A/V. While the stiffness variation of the isolators influences the acceleration response of the superstructure and the displacement response of the isolation system, the change in the fundamental periods is negligible.

To evaluate the torsional coupling caused by the dissimilarity in stiffness variations of the isolators, responses for the eccentric model, shown in Fig. 2(c), are investigated. Variations of ±10% for manufacturing and 10% for aging in the post-yield stiffness were assumed. Table 4 summarizes the maximum displacements at the top of the isolators for the eccentric model. The maximum displace-

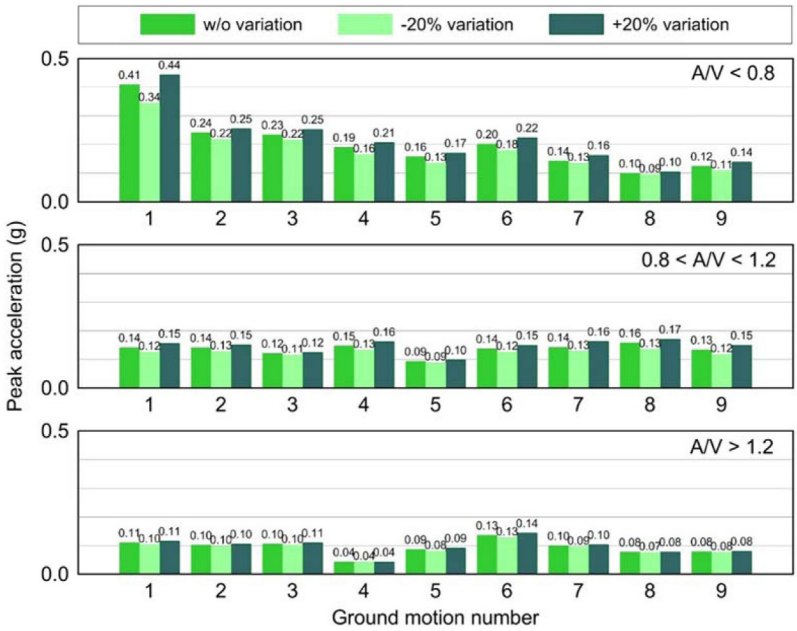

Fig. 5. Peak Acceleration at the Top of Superstructure for Stiffness Variations

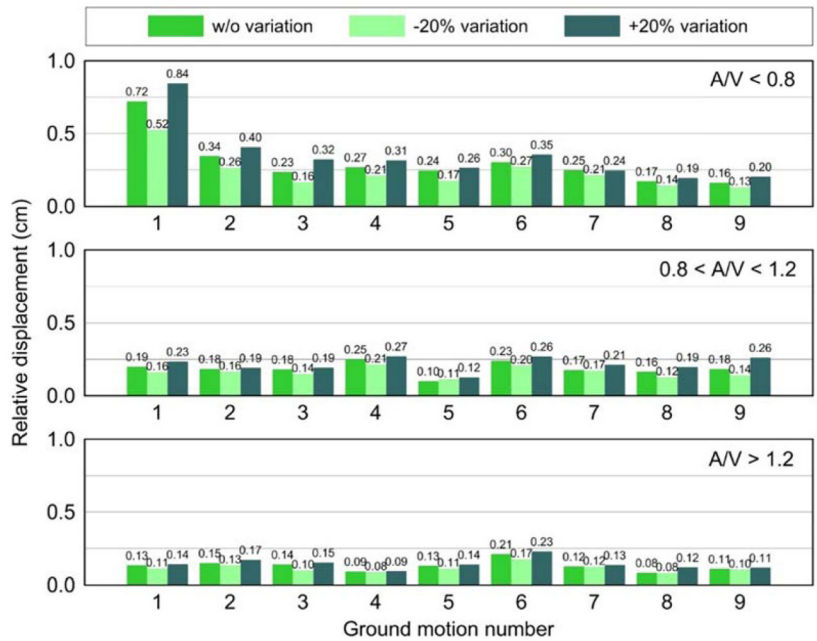

Fig. 6. Relative Displacement of Superstructure for Stiffness Variations

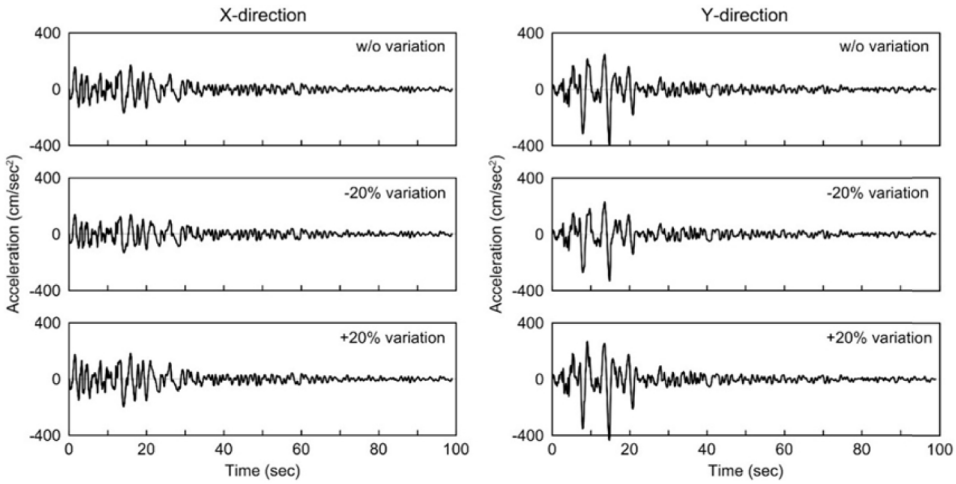

(a) Acceleration time-history at the top of superstructure

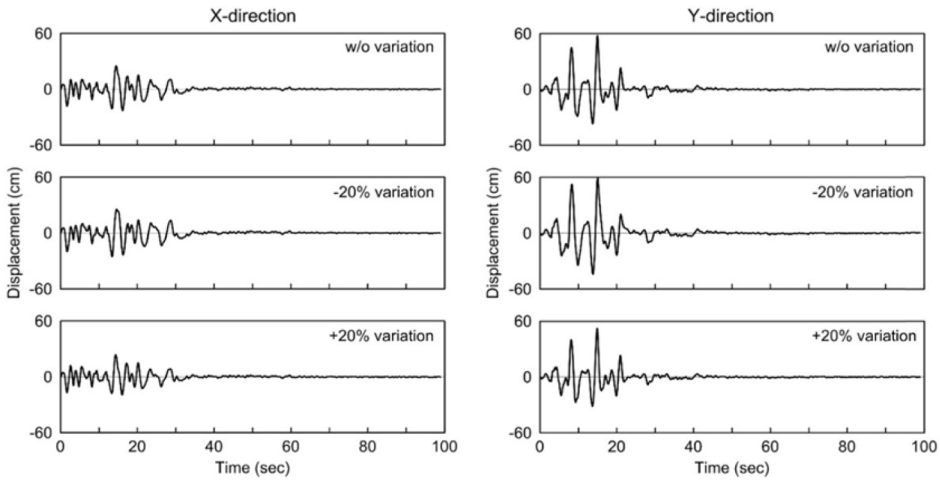

(b) Displacement time-history at the top of isolator

Fig. 7. Acceleration and Displacement Time-History in Superstructure and Isolator for EQ #1 in Low A/V

Table 4. Maximum Displacement at the Top of Isolators for Eccentric Model (cm)

EQ	A/V < 0.8		0.8 < A/V < 1.2		A/V > 1.2	
	Lateral Displ.	Vector Sum	Lateral Displ.	Vector Sum	Lateral Displ.	Vector Sum
1	60.76	64.76	10.52	10.98	3.75	4.35
2	35.07	39.54	12.25	12.78	5.77	6.36
3	35.67	40.54	13.28	15.27	3.41	3.75
4	26.81	28.83	20.02	20.14	0.88	1.06
5	22.12	23.53	3.10	3.14	3.60	4.70
6	30.46	30.78	13.86	16.93	10.42	10.67
7	21.72	22.25	17.46	19.05	2.49	2.61
8	8.01	8.20	13.62	14.91	4.40	6.09
9	9.17	9.17	14.06	14.41	3.21	3.24

ments of the isolators for the eccentric model increase up to 20% above the ideal model. Fig. 8 shows the ratios of peak displacements to the design displacement for the eccentric model. Variations in the manufacturing and aging processes of the isolators can influence the displacements of an isolation system for A/V < 1.2, but the effect of the variations can be neglected for ground motions with A/V > 1.2. For the eccentric model, the displacements and shear strains of the isolators due to individual variations are summarized in Table 5. Increases in the displacements and shear strains of the isolators are large for low A/V ratios. In general, the effect of the variation in the aging process on the displacement of the isolators is significant, and the effect of the variation in the operation temperature is considerable. For high A/V ratios, the effect of the eccentricity caused by the dissimilarity in the stiffness variations of isolators may be neglected.

The rotations of the isolation system due to stiffness and strength variations of the isolators can be neglected for ground motions with A/V > 0.8, but those for A/V < 0.8 cannot be ignored. For A/V < 0.8, the rotations were estimated to be up to 0.002 rad for the eccentric model.

The maximum shear force at the top of the isolators for the design and eccentric models are compared in Fig. 9. The shear force occurring at the top of the isolator increases significantly for the eccentric model. The increases of shear force for A/V < 0.8, 0.8 < A/V <1.2, and A/V >1.2 are up to 35.6%, 33.5%, and 17.5%, respectively.

Fig. 10 shows the effect of ambient temperatures on the shear strain of the isolators for EQ #1 at low A/V ratios. It can be observed that shear strains of the isolators are influenced by eccentricity and ambient temperature. Comparing Figs. 10(a) and 10(c), the shear strains at isolator B2 are increased to 295% from 227% in the X-direction, and increased to 552% from 527% in the Y-direction, due to the stiffness variability of the isolators. An increase in

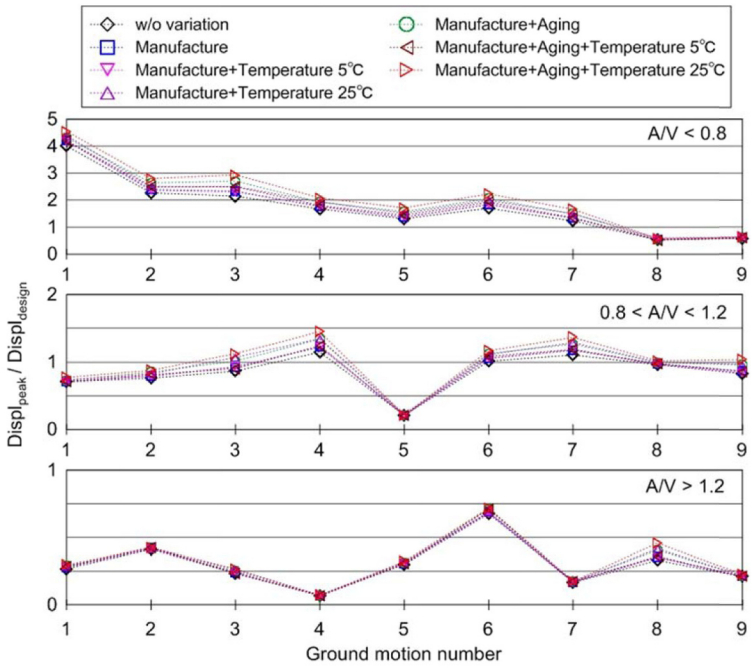

Fig. 8. Ratios of Maximum Displacements of Isolator for Eccentric Model

Table 5. Displacements and Shear Strains of Isolators due to Individual Variation for Eccentric Model

Variation	Low A/V				Intermediate A/V				High A/V			
	EQ #1		EQ #4		EQ #2		EQ #4		EQ #1		EQ #3	
	Displ. (cm)	Strain (%)	Displ. (cm)	Strain (%)	Displ. (cm)	Strain (%)	Displ. (cm)	Strain (%)	Displ. (cm)	Strain (%)	Displ. (cm)	Strain (%)
Manufacturing	2.95	26.82	1.38	12.55	0.43	3.91	1.16	10.55	0.15	1.36	0.06	0.52
Aging	1.78	16.18	2.42	22.00	0.92	8.36	1.74	15.82	0.17	1.55	0.18	1.64
Temperature	3.51	31.91	2.30	20.91	0.39	3.55	1.62	14.73	0.11	1.00	0.23	2.09

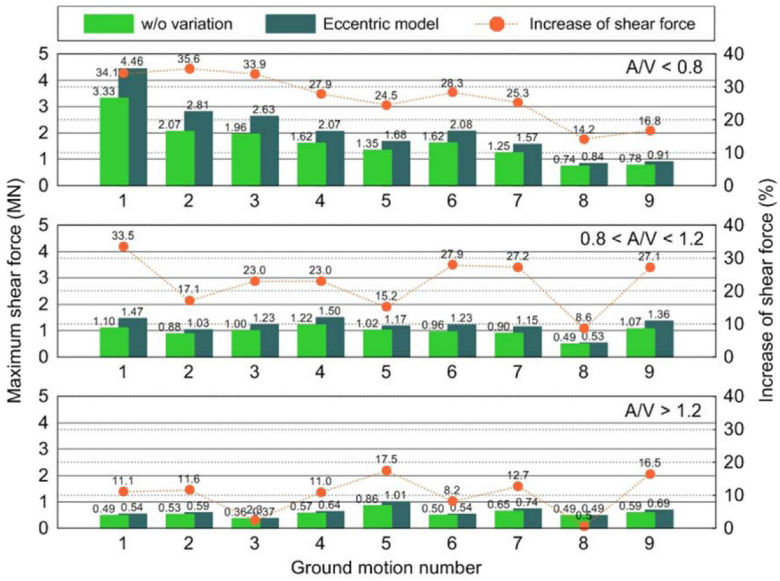

Fig. 9. Maximum Shear Forces at the Top of Isolators for Eccentric Model

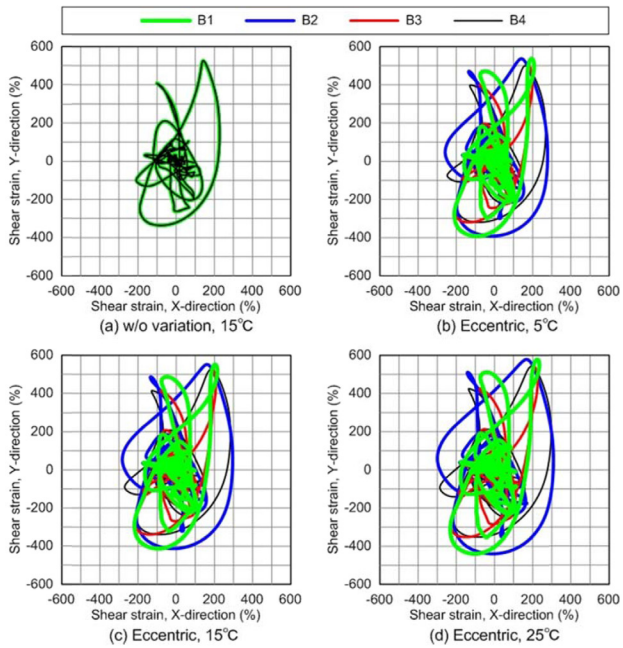

Fig. 10. Isolator Shear Strains for Different Ambient Temperatures (EQ #1 in Low A/V)

the ambient temperature from 15°C to 25°C causes an increase in shear strain from 295% to 309% in the X-direction, and from 552% to 578% in the Y-direction, as shown in Figs. 10(c) and 10(d).

Fig. 11 compares the maximum shear strains of the isolators for different variations. The effect of stiffness variation on the shear strain of the isolators is considerable, but the effect of eccentricity due to the dissimilarity in the stiffness variations of the isolators is not considerable. The shear strains of the isolators increase greatly at high temperatures because the stiffness and strength of the bearings decrease simultaneously for temperatures of higher than 15°C.

4. SUMMARY

This study investigated the effects of variability in the mechanical properties of LRBs on the response of seismically isolated structures for earthquake ground motions having different peak A/V ratios. The seismic response analysis of a base-isolated nuclear island, with or without eccentricity in the isolation system, was conducted using a stiffness variation of ±20%, which includes variations in the manufacturing and aging processes, as well as variation in the operating temperatures as addressed in ASCE-4 [25].

The seismic responses of the base isolation system and superstructure increase significantly for ground motions with low A/V ratios. The maximum displacements of the isolators for ground motions with A/V < 0.8 were up to four-times larger than those for ground motions with 0.8 < A/V < 1.2, which corresponds to the design response spectrum. The displacement of the isolators increases for the lower variation limit, i.e., -20%, but decreases for the upper variation limit, i.e., +20%. The upper and lower bounds are significant for A/V < 0.8, but negligible for A/V > 1.2. For A/V < 0.8, the isolators may be damaged or destroyed because their shear strains reach up to 600%. The variation in the mechanical properties of the isolators results in a significant influence on the shear strains of the isolators for ground motions with low A/V ratios. When displacements of the isolation system decrease, peak accelerations and relative displacements of the superstructure

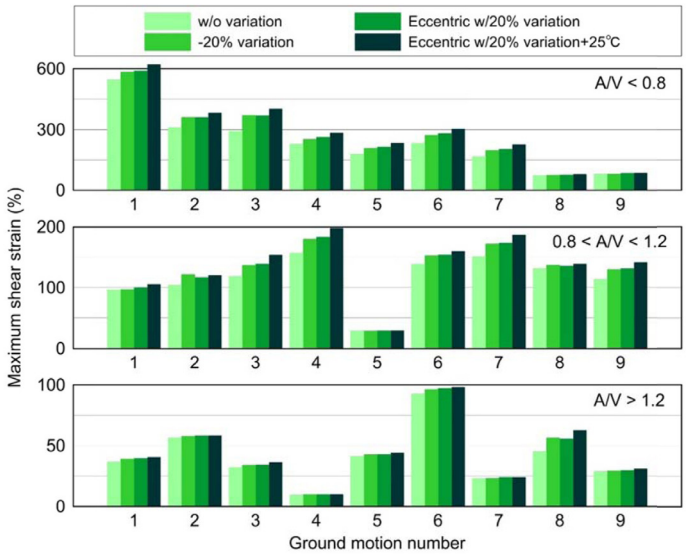

Fig. 11. Comparison of Maximum Shear Strains of Isolator for Different Variations

increase. For ground motions with low A/V ratios, the response of the superstructure increases remarkably. The effect of the stiffness variations of the isolators on the fundamental period of the base-isolated structure is negligible.

The eccentricity caused by the dissimilarity in the stiffness variations of the isolators results in a lateral-torsional coupling mode, and therefore increases the displacements and shear strains of the isolators. The effect of the eccentricity is not considerable for ground motions with intermediate and high A/V ratios, but the increase is significant for ground motions with low A/V ratios. In the eccentric model, the rotation and shear force of the isolators are increased by the eccentricity, especially at low A/V ratios. In general, the effect of the variation in the aging process on the displacement of the isolators is significant, and the effect of the variation in the operation temperature is considerable. High temperatures increase the shear strain of the isolators because the post-yield stiffness and strength of the isolators decrease simultaneously.

5. CONCLUSIONS

The investigation of the increase in responses of a seismically isolated structure due to variations in isolators and earthquake ground motions has led to the following conclusions:

1. The response of base isolated structures is very sensitive to the peak A/V ratios of earthquake ground motions. The increase in response is significantly amplified for ground motions with A/V < 0.6. The isolation system can be damaged or destroyed under peak ground accelerations less than the design level acceleration.
2. The increase in the response of an isolation system and superstructure due to variations in the mechanical properties of the isolators is considerable, except for ground motions with A/V > 1.2.
3. The variation provisions for the mechanical properties of isolators in the ASCE-4, which are ±20% over a 50- to 100-year period in the temperature range of 4.4°C (40°F) to 26.7°C (80°F), are adequate for normal ground motions. However, for isolation systems subjected to ground motions having rich low-frequency contents, especially for ground motions with A/V < 0.6, more strict variation limits should be given.
4. Variations in the mechanical properties of isolation system should be properly controlled during the manufacturing and aging processes for the application of isolation system to safety-related nuclear structures. Special consideration should be given to minimize the accidental torsion caused by the dissimilarity in stiffness variations of the isolators.
5. A clearance distance of the moat walls should be determined considering the characteristics of ground motions, i.e., peak A/V ratio, and the mechanical property variability of an isolation system during its lifetime. For isolation systems subjected to ground motions with low A/V ratios, moat walls and isolated structures should be designed to have increased distance or to resist large contact forces generated during pounding.

ACKNOWLEDGEMENT

This work was supported by the Nuclear Research & Development of the Korea Institute of Energy Technology Evaluation and Planning (KETEP) grant funded by the Korea government Ministry of Trade, Industry & Energy (No. 2011T100200080).

REFERENCES

[1] F. Naeim and J. M. Kelly, *Design of Seismic Isolated Structures: From Theory to Practice*, John Wiley & Sons, Inc., New York, NY, USA (1999).

[2] ASCE Standard ASCE/SEI 41-13, *Seismic Evaluation and Retrofit of Existing Buildings*, American Society of Civil Engineers, Reston, Virginia, USA (2014).

[3] J.C. Da la Llera and J.A. Inaudi, "Analysis of Base-Isolated Buildings Considering Stiffness Uncertainty in the Isolation System," *Proc. 5th U.S. National Conference on Earthquake Engineering*, Chicago, Illinois, Jul. 10-14, pp. 623-632, 1994.

[4] R.S. Jangid and J.M. Kelly, "Torsional Displacements in Base-Isolated Buildings," *Earthquake Spectra*, vol. 16, pp. 443-454 (2000).

[5] S. Nagarajaiah, A.M. Reinhorn, and M.C. Constantinou, "Torsion in Base-Isolated Structures with Elastomeric Isolation Systems," *Journal of Structural Engineering*, vol. 119, pp. 2932-2951 (1993).

[6] A. Tena-Colunga and C. Zambrana-Rojas, "Dynamic Torsional Amplifications of Base-Isolated Structures with an Eccentric Isolation System," *Engineering and Structures*, vol. 28, pp. 72-83 (2006).

[7] V. A. Matsagar and R. S. Jangid, "Base-isolated Building with Asymmetries due to the Isolator Parameters," *Advances in Structural Engineering*, vol. 8, pp. 603-621 (2005).

[8] W. K. Tso, T. J. Zhu, and A. C. Heidebrecht, "Engineering Implication of Ground Motion A/V Ratio," *Soil Dynamics and Earthquake Engineering*, vol. 11, pp. 133-144 (1992).

[9] H. Sucuoglu, S. Yücemen, A. Gezer, and A. Erberik, "Statistical Evaluation of the Damage Potential of Earthquake Ground Motions," *Structural Safety*, vol. 20, pp. 357-378 (1998).

[10] Y. S. Choun, "Sloshing Response of Liquid Storage Tanks Subjected to Earthquakes with Different Peak Acceleration to Velocity Ratios," *Proc. 15th World Conference on Earthquake Engineering*, Lisboa, Portugal, Sep. 24-28, 2012.

[11] A. Shirazi, "Thermal Degradation of the Performance of Elastomeric Bearings for Seismic Isolation," *Ph. D. Dissertation*, University of California, San Diego, USA (2010).

[12] M. C. Constantinou, A. S. Whittaker, Y. Kalpakidis, D. M. Fenz, and G. P. Warn, "Performance of Seismic Isolation Hardware under Service and Seismic Loading," MCEER-07-0012, Multidisciplinary Center for Earthquake Engineering Research (2007).

[13] ISO 22762-3, "Elastomeric Seismic-Protection Isolators. Part 3: Applications for Buildings – Specifications," International Standard (2010).

[14] T. A. Morgan, A. S. Whittaker, and A. C. Thompson, "Cyclic Behavior of High-Damping Rubber Bearings," *Proc. 5th World Congress on Joints, Bearings and Seismic Systems for Concrete Structures*, American Concrete Institute, Rome, Italy, Oct. 7-11, 2001.

[15] H. Gu and Y. Itoh, "Aging Behaviors of Natural Rubber in Isolation Bearings," *Advanced Material Research*, vols. 163-167, pp. 3343-3347 (2011).

[16] M. Kato, Y. Watanabe, G. Yoneda, E. Tanimoto, T. Hirotani, K. Shirahama, Y. Fukushima, and Y. Murazumi, "Investigation of Aging Effects for Laminated Rubber Bearings of Pelham Bridge," *Proc. 11th World Conference on Earthquake Engineering*, Paper No. 1450, Acapulco, Mexico, Jun. 23-28, 1996.

[17] H. Hamaguchi, Y. Samejima, and N. Kani, "A Study of Aging Effect on Rubber Bearings After About Twenty Years in Use," *Proc. 11th World Conference on Seismic Isolation, Energy Dissipation and Active Vibration Control of Structures*, Guangzhou, China, Nov. 17-21, 2009.

[18] I. Shimoda, I. Masayoshi, M. Mochimaru, M. Miyazaki, S. Sakuraba, K. Masuda, and T. Wake, "Survey of Aging for LRB of a Base-Isolated Building Completed 15 Years Ago," *PVP-Vol. 486-2, Seismic Engineering - 2004*, San Diego, California, Jul. 25-29, 2004.

[19] C. Coladant, "Durability and Aging of Elastomeric Bearings in France," *Proc. Int. Post-SMiRT Conference Seminar on Isolation, Energy Dissipation and Control of Vibrations of Structures*, Capri (Napoli), Italy, Aug. 23-25, 1993.

[20] P. Labbé, "Pioneering Actual Use of Seismic Isolation for Nuclear Facilities," *1st Kashiwazaki Int. Symposium on Seismic Safety of Nuclear Installations: JNES/EDF Workshop on Seismic Isolation of Nuclear Facilities*, Kashiwazaki, Japan, Nov. 24-26, 2010.

[21] AASHTO, "Guide specifications for seismic isolation design," American Association of State Highway and Transportation Officials, Washington, D.C. (1999).

[22] C. W. Roeder, J. F. Stanton, and A. W. Taylor, "Performance of Elastomeric Bearings," Report No. 298, National Cooperative Highway Research Program, Transportation Research Board, Washington, D.C. (1987).

[23] M. C. Constantinou, P. Tsopelas, A. Kasalanati, and E. D. Wolff, "Property Modification Factors for Seismic Isolation Bearings," MCEER-99-0012, Multidisciplinary Center for Earthquake Engineering Research, State University of New York, Buffalo, NY (1999).

[24] O. Hasegawa, I. Shimoda, and M. Ikenaga, "Characteristic of Lead Rubber Bearing by Temperature," *Summaries of Technical Papers of Annual Meeting Architectural Institute of Japan, B-2, Structures II, Structural Dynamics Nuclear Power Plants*, Architectural Institute of Japan, pp. 511-512, 1997 (in Japanese).

[25] ASCE-4 Draft, *Seismic Analysis of Safety-Related Nuclear Structures and Commentary*, American Society of Civil Engineers, Reston, Virginia, USA (2013).

[26] Regulatory Guide 1.60, "Design Response Spectra for Seismic Design of Nuclear Power Plants," U.S. Nuclear Regulatory Commission, Washington, D.C. (1973).

[27] N. Naumoski, W. K. Tso, and A. C. Heidebrecht, "A Selection of Representative Strong Motion Earthquake Records having Different A/V Ratios," EERG Report 88-01, Earthquake Engineering Research Group, McMaster University, Hamilton, Ont., Canada (1988). also, http://www.caee.uottawa.ca/Publications/Earthquake%20records/Earthquake%20Records.htm.

[28] Bridgestone Corp., Seismic Isolation Product Line-up, pp. 8-9 (2013).

[29] Y. N. Huang, A. S. Whittaker, R. P. Kennedy, and R. L. Mayes, "Assessment of Base-Isolated Nuclear Structures for Design and Beyond-Design Basis Earthquake Shaking," MCEER-09-0008, Multidisciplinary Center for Earthquake Engineering Research, State University of New York, Buffalo, NY (2009).